Steady-State and Pre-Steady-State Kinetic Analysis of dNTP Insertion Opposite 8-Oxo-7,8-dihydroguanine by *Escherichia coli* Polymerases I exo$^-$ and II exo$^-$ †

Laura G. Lowe and F. Peter Guengerich*

Department of Biochemistry and Center in Molecular Toxicology, Vanderbilt University School of Medicine, Nashville, Tennessee 37232-0146

Received February 27, 1996; Revised Manuscript Received May 8, 1996⊗

ABSTRACT: *Escherichia coli* polymerases (pol) I exo$^-$ (KF$^-$) and pol II exo$^-$ (pol II$^-$) were used as model enzymes with a DNA primer/template complex (12/16-mer) to examine the kinetics of incorporation of dCTP and dATP at the site of an 8-oxo-7,8-dihydroguanine (8-oxoGua) residue, compared to guanine (Gua). In steady-state assays (with DNA in excess) the rate of incorporation (k_{cat}) was dCTP > dATP and the $K_{m,dATP} < K_{m,dCTP}$ during incorporation opposite 8-oxoGua with both polymerases. Pre-steady-state kinetic curves (rapid-quench analysis) for the addition of C opposite 8-oxoGua or Gua by KF$^-$ and pol II$^-$ were all biphasic, with a rapid initial single-turnover burst followed by a slower multiple turnover rate, while addition of A opposite 8-oxoGua did not display burst kinetics with either enzyme. Reduced rates of incorporation of the dCTPαS and dATPαS phosphorothioate analogs suggest that the rates of incorporation of A and C opposite 8-oxoGua are limited during polymerization by the rate of phosphodiester bond formation. Neither polymerase appears to discriminate between adducted and nonadducted DNA substrate for binding. Kinetic assays performed with varying dCTP concentrations indicate that dCTP has a higher K_d and lower k_p (polymerization rate) for incorporation opposite 8-oxoGua compared to Gua. Furthermore, the dATP binding affinities with KF$^-$ and pol II$^-$ were ∼10- and ∼3-fold lower, respectively, than that of dCTP as determined in competition assays with mixtures of dCTP and dATP. Microscopic rate constants were estimated by mathematical analysis of dNTP concentration dependence curves. Both polymerases preferentially extended the A:8-oxoGua pair while extension of the C:8-oxoGua pair was greatly impaired. Based on these findings, the fidelity of KF$^-$ and pol II$^-$ during replication of 8-oxoGua depends on contributions from nucleotide binding, the rate of phosphodiester bond formation, and the ease of base pair extension.

DNA modifications resulting from exogenous and endogenous reactions with chemicals and oxygen are precursors to mutagenic events (Basu & Essigmann, 1988; Ames & Gold, 1991; Cheng et al., 1992). The mutagenicity of DNA adducts partly arises from their miscoding properties when the DNA is replicated by a polymerase (Basu & Essigmann, 1988, 1990; Feig & Loeb, 1994). Thus, polymerase fidelity during DNA replication is a major contributor to the prevention of mutagenesis and consequently carcinogenesis.

The modified DNA base adduct 8-oxo-7,8-dihydroguanine (8-oxoGua)[1] is produced by both endogenous and exogenous reactive oxygen species and causes G to T transversions when replicated (Ames et al., 1993; Marnett & Burcham, 1993). 8-OxoGua is found at levels of 10−250 molecules per 10^6 guanines in some mammalian tissues and is the most common DNA lesion formed from reactive oxygen species (Ames et al., 1993). Increased levels of 8-oxoGua have been associated with chronic hepatitis in human liver (Shimoda et al., 1994), with oxidative damage in human leukocytes (Takeuchi et al., 1994), and with human breast cancer (Malins & Haimanot, 1991; Malins et al., 1993, 1995).

Melting studies of DNA duplexes containing 8-oxoGua:C and 8-oxoGua:A base pairs reveal that the T_m for the 8-oxoGua:A pair is only 6 °C lower than the T:A normal base pair while the T_m for the 8-oxoGua:C pair is more than 35 °C lower than that for the G:C base pair (McAuley-Hecht et al., 1994). Thus, insertion of an A (instead of C) across from an 8-oxoGua moiety might be expected to be favored on thermodynamic grounds. On the basis of X-ray crystallographic and NMR structures of 8-oxoGua:A and 8-oxoGua:C base pairs, the miscoding potential of 8-oxoGua has been proposed to be due to the similarity of an 8-oxoGua:A base pair to the Watson−Crick canonical T:A base pair (Kouchakdjian et al., 1991; McAuley-Hecht et al., 1994; Lipscomb et al., 1995).

The kinetic parameters K_m and k_{cat} for insertion opposite and extension of 8-oxoGua were previously determined by steady-state techniques with KF$^+$ and DNA polymerase α (Shibutani et al., 1991). With KF$^+$, the changes in K_m values were more significant than changes in V_{max} during the insertion of dCTP or dATP opposite 8-oxoGua, compared to insertion of dCTP opposite Gua. Likewise, with DNA polymerase α larger changes were noted in K_m than V_{max}, although the V_{max} for insertion of dCTP opposite 8-oxoGua was reduced to a greater extent than seen with KF$^+$.

† This work was supported in part by United States Public Health Service (USPHS) Grants CA44353 and ES00267. L.G.L. was supported in part by USPHS Training Grant ES07028.

* Author to whom correspondence should be addressed.

⊗ Abstract published in *Advance ACS Abstracts,* July 1, 1996.

[1] Abbreviations: 8-oxoGua, 8-oxo-7,8-dihydroguanine; dNTPαS, α-thiodeoxynucleoside triphosphate; EDTA, (ethylenedinitrilo)tetraacetic acid; FABMS, fast atom bombardment mass spectrometry; Gua, guanine; HIV-1, human immunodeficiency virus-1; KF$^+$, *Escherichia coli* polymerase I (Klenow fragment) exo$^+$; KF$^-$, *E. coli* pol I (Klenow fragment) exo$^-$; pol II$^-$, *E. coli* polymerase II exo$^-$; Tris, tris(hydroxymethyl)aminomethane; DTT, dithiothreitol.

S0006-2960(96)00485-0 CCC: $12.00

Scheme 1: General Catalytic Mechanism for DNA Polymerases (Johnson, 1993)[a]

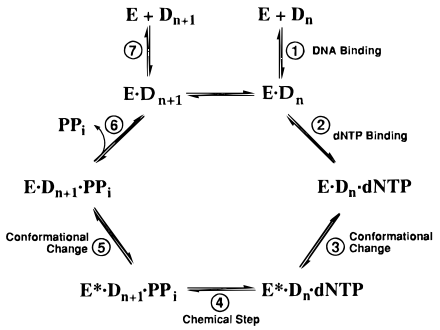

[a] Steps for a distributive enzyme are numbered. The assays in this study allow only for a single round of nucleotide addition followed by substrate release (step 7). A processive enzyme continues through multiple rounds of nucleotide addition before releasing the DNA substrate when dNTPs are present that can be added at sites beyond the first one. Abbreviations: E = polymerase; D_n = DNA; E* = conformational change in polymerase; and D_{n+1} = DNA extended by one base.

Despite these observations concerning the kinetics of extension of the 8-oxoGua adduct, the direct meaning of K_m in steady-state experiments with processive polymerases is not clear. Single-turnover analysis allows evaluation of the microscopic steps governing polymerization (Scheme 1) (Johnson, 1992) and the contributions of individual steps to observed mutational spectra and therefore provides a more complete understanding of the events involved in polymerase fidelity and mutagenesis. Two previous papers in this area have described the pre-steady-state kinetics of polymerization of O^6-methylguanine by KF^+ (Tan et al., 1994) and of C^8-2-acetylaminofluorenyl and 2-aminofluorenyl Gua adducts by T7 DNA polymerase exo$^-$ (Lindsley & Fuchs, 1994). Tan et al. (1994) found that during insertion of dCTP, the "correct" base, opposite O^6-methylguanine the rate of phosphodiester bond formation was 5-fold less than insertion of dTTP. However, no experiments with dCTP opposite Gua were reported for comparison.

In this paper, the mechanisms of polymerization of nonadducted and 8-oxoGua-adducted sequences were examined by rapid kinetic analysis and compared in order to identify the elementary steps of polymerization that are most important for mutagenesis and fidelity. The polymerases used in this study, *Escherichia coli* DNA polymerases I and II, are exonuclease deficient (exo$^-$). Pol II$^-$ is a single 90-kDa polypeptide and is a member of the group B ("α-like") polymerase family. Functionally, pol II$^-$, like KF$^-$, is involved primarily in DNA repair (Kornberg & Baker, 1992). Many details of the catalytic mechanism for stepwise polymerization by KF$^-$ have been elucidated (Bryant et al., 1983; Eger & Benkovic, 1992; Kuchta et al., 1988; Eger et al., 1991), but pol II$^-$ has not been studied in this manner. The results of our analysis provide the first description of individual rate constants governing replication of 8-oxoGua by polymerases.

EXPERIMENTAL PROCEDURES

Enzymes. The CJ375 overproducer strain for *E. coli* KF$^-$ (D355A,E357A) was provided by Dr. C. Joyce (Yale University, New Haven, CT). KF$^-$ was purified to electrophoretic homogeneity (Laemmli, 1970) as described by Joyce and Grindley (1983) and modified by Derbyshire et al. (1988). Protein concentrations were determined using ϵ_{280} = 6.32 × 10^4 M^{-1} cm^{-1}. Purified KF$^-$ was stored in small aliquots at −70 °C in 50 mM Tris-HCl (pH 7.5) buffer containing 50% glycerol (v/v) and 0.5 mM DTT. Dr. M. Goodman (University of Southern California, Los Angeles, CA) provided the pHC700 overproducing plasmid for the *E. coli* DNA pol II$^-$ (D155A/E157A). The plasmid was transfected into *E. coli* JM109 cells to overproduce the enzyme, which was purified as described (Cai et al., 1995). Protein concentrations were determined using ϵ_{280} = 12.4 × 10^4 M^{-1} cm^{-1}.[2] Purified pol II$^-$ was also stored in small aliquots at −70 °C in 10 mM Tris-HCl (pH 7.4) buffer containing 50% glycerol (v/v), 150 mM NaCl, 1 mM EDTA, and 1 mM DTT.

Table 1: Oligonucleotides[a]

control 12/16-mer	5′- CCGCAGACGCAG
	3′- GGCGTCTGCGTCGCTC
8-oxoGua modified 12/16-mer	5′- CCGCAGACGCAG
	3′- GGCGTCTGCGTCXCTC
8-oxoGua modified 13A/16-mer	5′- CCGCAGACGCAGA
	3′- GGCGTCTGCGTCXCTC
8-oxoGua modified 13C/16-mer	5′- CCGCAGACGCAGC
	3′- GGCGTCTGCGTCXCTC

[a] X denotes the position of 8-oxoGua.

Nucleoside Triphosphates. Unlabeled Ultrapure Grade dNTPs were purchased from Pharmacia Biotech (Uppsala, Sweden), (S_p)-dNTPαSs were purchased from United States Biochemical Corp. (Cleveland, OH), and [γ-^{32}P]ATP was purchased from DuPont-New England Nuclear (Boston, MA).

Oligonucleotide Synthesis. All oligonucleotides (Table 1) were synthesized on an automated Applied Biosystems 391 DNA synthesizer (Applied Biosystems/Perkin Elmer, Foster City, CA). Chemicals for oligonucleotide synthesis, except the 8-oxoGua phosphoramidite, were purchased from Cruachem Ltd. (Glasgow, U.K.). Oligonucleotides were sequentially purified by reversed-phase HPLC and gel electrophoresis. For HPLC purification, a Beckman Ultrasphere octadecylsilane column (San Ramon, CA) was used with gradients composed of 0.10 M $NH_4CH_3CO_2$ (pH 7.5) or 0.10 M triethylammonium acetate (pH 7.4) and 90% aq CH_3CN (v/v), with increasing CH_3CN. In some cases oligonucleotides were further separated by gel electrophoresis [20% acrylamide (w/v), 1.5% bisacrylamide (w/v), and 8.0 M urea in 90 mM Tris-borate (pH 8.0) containing 2 mM EDTA], bands were excised from the gels, the DNA was eluted by crushing the gel and shaking overnight in water, and the oligonucleotides were recovered by C_2H_5OH precipitation. Concentrations of purified oligonucleotides were estimated by UV absorbance at 260 nm on a modified Cary-14/OLIS spectrophotometer (On-Line Instrument Systems, Bogart, GA). Extinction coefficients were as follows: 12-mer, ϵ = 121 700 M^{-1} s^{-1}; 16-mer, ϵ = 142 500 M^{-1} cm^{-1}; 13-mer with 3′-A, ϵ = 128 000 M^{-1} s^{-1}; and 13-mer with 3′-C, ϵ =120 400 M^{-1} s^{-1} (Boyer, 1975).

Preparation of 8-OxoGua Phosphoramidite and Site-Specifically Modified Oligonucleotide. Synthesis of the 8-oxoGua phosphoramidite from 2′-deoxyguanosine was accomplished as described by Bodepudi et al. (1992). Briefly, 2′-deoxyguanosine (**1**) was treated with saturated Br_2/

[2] W. F. Anderson, personal communication.

H_2O, giving a 54% yield of 8-bromo-2′-deoxyguanosine (**2**) which was used to produce 8-benzyloxy-2′-deoxyguanosine (**3**) in a solution of $(CH_3)_2SO$ and sodium benzoylate (54% yield) (mp 204−205 °C, lit. 201 °C; FABMS *m/z* 396.1 MH^+Na^+). Proton (300 MHz) NMR spectra of product **3** were recorded (Bruker AC300 spectrometer, Bruker, Billerica, MA) $(C^2H_3)_2SO$: δ 7.29−7.48 [5 H, aromatic H, m], 6.45 [2 H, NH_2, s], 6.03−6.14 [1 H, H-C(1′), t], 5.39 [2 H, CH_2-Ph, s], 5.16 [1 H, OH-C(3′), d], 4.89 [1 H, OH-C(5′), m], 4.39 [1 H, H-C(3′), m], 3.71 [1 H, H-C(4′), m], the 2 H, H-C(5′) peaks obscured by H_2O contamination, 2.78−2.88 [1 H, H-C(2′), m], 2.03 [1 H, H-C(2″), m]. Product **3** was isobutyrylated using trimethychlorosilane and isobutyric anhydride to give 8-benzyloxy-N^2-isobutyryl-2′-deoxyguanosine (**4**) (73% yield). Hydrogenation over 10% Pd-charcoal catalyst gave a 91% yield of 7,8-dihydro-N^2-isobutyryl-8-oxo-2′-deoxyguanosine (**5**) (FABMS MH^+ 354.2). 7,8-Dihydro-5′-*O*-(4,4′-dimethoxytrityl)-N^2-isobutyryl-8-oxo-2′-deoxyguanosine (**6**) was prepared by treatment of (**5**) with 4,4′-dimethyltrityl chloride (46% yield) and recovered by chromatography over silica gel using 0.5% CH_3OH in CH_2Cl_2 (v/v). After evaporation twice from dry CH_2Cl_2 and benzene, product **6** was reacted with 2-cyanoethyl *N*,*N*-diisopropylphophoramidochloridite to yield 3′-*O*-[(diisopropylamino)(2-cyanoethoxy)phosphino]-7,8-dihydro-5′-*O*-(4,4′-dimethoxytrityl) (**7**). The 8-oxoGua phosphoramidite (**7**) was filtered under N_2, evaporated, and dried *in vacuo* over P_2O_5 prior to addition of DNA synthesis grade anhydrous CH_3CN (Applied Biosystems). The coupling efficiency of the phosphoramidite in the 16-mer sequence (3′-GGCGTCT-GCGTCXCTC-5′, where X = 8-oxoGua) was >95% as determined by measurement of absorbance of trityl solution wastes from the DNA synthesizer. The resulting oligonucleotide was purified as described. The presence of the 8-oxoGua in the 16-mer sequence was confirmed by electrospray negative-ion mass spectrometry by Dr. A. K. Chaudhary in the Vanderbilt facility: theo. MH^+ 4877.77; found 4879.08. Mass spectrometry of the control 16-mer containing Gua instead of 8-oxoGua yielded MH^+ 4864.35 (theo. 4862.72).

Primer End Labeling and Primer/Template Annealing. Primers were 5′-end-labeled by T4 polynucleotide kinase (Gibco BRL Life Technologies, Grand Island, NY) with [γ-^{32}P]ATP (3000 Ci/mmol) as previously described (Boosalis et al., 1987). Following kinase inactivation at 65 °C, unreacted [γ-^{32}P]ATP was separated from labeled primer on a spin column prepared with Sephadex G-10 (Pharmacia). Annealing was accomplished by denaturation of a 1:1.5 molar ratio of primer:template at 85−100 °C for 2 min followed by slow cooling over 1−2 h to ambient temperature.

Steady-State Incorporation of dCTP or dATP Opposite Gua or 8-OxoGua. Steady-state reactions with KF^- and unmodified 12/16-mer (control template) contained 0.08 nM KF^- and 41 nM primer/template duplex (final concentrations). KF^- steady-state reactions with the 8-oxoGua-modified 12/16-mer contained 0.15 nM KF^- and 41 nM duplex DNA (final concentrations). Reactions with pol II$^-$ and the Gua-containing template contained 1.0 nM pol II$^-$ and 41 nM duplex DNA while reactions with the 8-oxoGua-containing template contained 5.0 nM pol II$^-$ and 41 nM duplex DNA (final concentrations). Reactions were initiated by the addition of an equal volume of dNTP (varying concentrations) in 100 mM Tris-HCl buffer (pH 7.4) containing 25 mM $MgCl_2$ (buffer A) (final concentrations of Tris-HCl and $MgCl_2$ were 50 and 12.5 mM, respectively). Reactions were quenched after 5.0 min with twice the reaction volume of 20 mM EDTA, pH 7.4 (13.3 mM final concentration). All steady-state reactions contained 50 mM Tris-HCl (pH 7.4) buffer with 12.5 mM $MgCl_2$ and 1.0 mM EDTA in 8.0 μL total volume and were done in triplicate. Products were analyzed by electrophoresis on a denaturing gel [16% acrylamide (w/v), 1.5% bisacrylamide (w/v) and 8.0 M urea]. A k•cat kinetic program (BioMetallics Inc., Princeton, NJ) was used to determined the steady-state parameters (K_m and k_{cat}) and associated residual variance for incorporation of dCTP opposite Gua and dCTP and dATP opposite 8-oxoGua for each polymerase following visualization and quantitation of extended 12-mer product using a Molecular Dynamics PhosphorImager (model 400E, Molecular Dynamics Inc., Sunnyvale, CA) and ImageQuant software version 3.3.

Rapid Quench Experiments. Pre-steady-state (rapid quench) experiments were carried out in a KinTek Quench-Flow Apparatus (Model RQF-3, KinTek Corp., State College, PA), which had been calibrated (loop volumes) with ^{32}P according to the manufacturer's instructions. Reactions were started by rapid mixing of primer/template/polymerase mixture (19.4 μL) with either dCTP or dATP in buffer A (21.5 μL) and then quenched with 0.6 M EDTA, pH 7.4. Products were analyzed by gel electrophoresis and quantitated as described above.

Competition Assays. Competition assays with dCTP and dATP were done to approximate the $K_{d,app}$ values for polymerase binding of dATP in reactions with 8-oxoGua-containing template. The assays were performed using the general approach described above for the rapid-quench experiments, except that the dNTP solution contained both dCTP and dATP at varying concentrations. Reactions were done with the following final concentration combinations of dCTP and dATP: 20 μM dCTP/20 μM dATP; 20 μM dCTP/60 μM dATP; 20 μM dCTP/200 μM dATP; 60 μM dCTP/20 μM dATP; 60 μM dCTP/60 μM dATP; 60 μM dCTP/200 μM dATP; and 200 μM dCTP/200 μM dATP. Products were analyzed by electrophoresis as described earlier, except that 20% acrylamide/8.0 M urea gels were used. Bands corresponding to primer extended by C and A could be resolved under these conditions and quantitated in the usual way (*vide infra*).

Measurement of Extension Past C:8-oxoGua, A:8-oxoGua, C:G, and A:C pairs. Rapid quench experiments were done to determine the efficiency of extension past an 8-oxoGua base pair with a 13-mer primer containing either an A or a C in the 3′-position opposite 8-oxoGua. All reactions were initiated by rapid mixing of the primer/template/enzyme solution with 200 μM dGTP (final concentration) in buffer A. Products were analyzed as described above.

Kinetic Simulations. In order to estimate the rate constants governing Scheme 1, kinetic simulations modeling the observed kinetic curves for dNTP incorporation were done by mathematical analysis using HopKINSIM version 1.7, obtained from Dr. Carl Freiden (Washington University, St. Louis, MO) (Barshop et al., 1983) on a Macintosh Power PC 7100 computer (Apple Computer Inc., Cupertino, CA) equipped with SoftwareFPU version 3.03 (John Neil & Associates, Cupertino, CA).

Computer Graphing Programs. Graphs shown were generated in either CA-Cricket Graph III version 1.5 (Computer Associates International, Inc., Islandia, NY) or

Table 2: Steady-State Kinetic Parameters for KF$^-$ and Pol II$^-$

	KF$^-$		pol II$^-$	
	K_m (μM)	k_{cat} (s^{-1})	K_m (μM)	k_{cat} (s^{-1})
G:C[a]	1.1 ± 0.2	0.37 ± 0.02	0.44 ± 0.06	0.048 ± 0.002
8-oxoG:C[a]	28 ± 12	0.33 ± 0.10	22 ± 4	0.0083 ± 0.0003
8-oxoG:A[a]	1.7 ± 1.3	0.005 ± 0.001	11 ± 1	0.0040 ± 0.0002
f[b]	0.3		1.0	

[a] The base in the oligomer is presented first (G or 8-oxoGua), followed by the dNTP used. [b] The apparent misinsertion frequency is defined as $f = [(V_{max}/K_m)_{dATP}/(V_{max}/K_m)_{dCTP}]$ (Boosalis et al., 1987, 1989), with substitution of k_{cat} for V_{max} in this work.

KaleidaGraph version 3.0.5 (Synergy Software, Reading, PA). KaleidaGraph software is equipped with nonlinear regression routines and error analysis which provide a best fit of the data to equations describing the data (these equations are indicated in the figure legends and text).

RESULTS

Steady-State Kinetics of dCTP and dATP Incorporation Opposite 8-OxoGua and dCTP Incorporation Opposite Gua. Steady-state assays with KF$^-$ and unmodified or 8-oxoGua-modified 12/16-mers were carried out with ~500- and ~300-fold excesses of DNA over enzyme, respectively (Table 2). Insertion of dCTP opposite either Gua or 8-oxoGua yielded a similar k_{cat} value (0.37 ± 0.02 s^{-1} and 0.33 ± 0.10 s^{-1}, respectively) while the K_m for insertion of dCTP opposite 8-oxoGua was ~30 times higher than K_m for insertion of dCTP opposite Gua (28 ± 12 μM vs 1.1 ± 0.2 μM, respectively). For insertion of dATP opposite 8-oxoGua, the K_m was similar to that for insertion of dCTP opposite Gua (1.7 ± 1.3 μM), but the k_{cat} was reduced by two orders of magnitude (0.005 ± 0.001 s^{-1}). After the 5 min incubation time, insertion of dATP opposite Gua could not be detected for comparison of dCTP insertion because the rate was too low. The misinsertion frequency (f) of KF$^-$ in this context was determined to be 0.3 by the relationship $f = [(k_{cat}/K_m)_{dATP}/(k_{cat}/K_m)_{dCTP}]$ (Boosalis et al., 1987, 1989). This translates into a fidelity of 3.5, or ~30% estimated misinsertion of dATP opposite 8-oxoGua.

Steady-state assays with pol II$^-$ and unmodified or 8-oxoGua-modified 12/16-mers were carried out with ~40- and ~8-fold excesses of DNA over enzyme, respectively (Table 2). Insertion of dCTP opposite 8-oxoGua yielded k_{cat} and K_m values (0.0083 ± 0.0003 s^{-1} and 22 ± 4 μM) different from those for insertion of dCTP opposite Gua (0.048 ± 0.002 s^{-1} and 0.44 ± 0.06 μM). The k_{cat} and K_m values for insertion of dATP opposite 8-oxoGua (0.0040 ± 0.0002 s^{-1} and 11 ± 1 μM) were similar to those for insertion of dCTP opposite 8-oxoGua. Insertion of dATP opposite Gua could not be measured for comparison. The fidelity of pol II$^-$ was determined to be ~1.0, indicating 50% misinsertion frequency of dATP opposite 8-oxoGua.

Pre-Steady-State Kinetics of dCTP and dATP Incorporation Opposite 8-OxoGua and dCTP Incorporation Opposite Gua. Pre-steady-state experiments were done with 3−5-fold excess of DNA over enzyme. Reactions were initiated by the rapid mixing of enzyme preincubated with 12/16-mer and a solution of dNTP and $MgCl_2$ and then quenched by the addition of 0.3 M EDTA (pH 7.4) over a time range varying from 5 ms to 10 s. With KF$^-$, the pre-steady-state incorporation of dCTP opposite unmodified 12/16-mer is shown in Figure 1A, in comparison to incorporation of dCTP (Figure 1B) or dATP (Figure 1C) opposite 8-oxoGua in the modified 12/16-mer. The solid lines represent a fit of the data to the kinetic mechanism shown in Scheme 1 for a distributive enzyme and the rate constants shown in Table 3. There is a fast phase (burst) for addition of dCTP opposite Gua and 8-oxoGua but not for addition of dATP opposite 8-oxoGua, suggesting that the rate-limiting step for addition of dATP by KF$^-$ occurs at or before the chemical step.

Pre-steady-state incorporation of dCTP by pol II$^-$ opposite unmodified 12/16-mer is shown in Figure 1D, in comparison to incorporation of dCTP (Figure 1E) or dATP (Figure 1F) opposite 8-oxoGua in the modified 12/16-mer. The solid lines represent a fit of the data to the kinetic mechanism shown in Scheme 1 and the rate constants shown in Table 3. A burst of product formation was seen for addition of dCTP opposite Gua and a smaller burst for addition of dCTP opposite 8-oxoGua, but no burst was observed for addition of dATP opposite 8-oxoGua.

Phosphorothioate Elemental Analysis. In order to address the hypothesis that the chemical step is the rate-limiting step in the catalytic mechanism of KF$^-$ and pol II$^-$, the normal dNTPs were replaced with their phosphorothioate analogs (Figure 1). The substitution of dCTPαS for dCTP had no effect on the rate of product formation with KF$^-$ and unmodified 12/16-mer (Figure 1A). However, incorporation of dCTPαS or dATPαS opposite 8-oxoGua-modified 12/16-mer diminished the rate of product formation by KF$^-$ (Figure 1B,C). The elemental effects were ~1, ~35, and ~20 for incorporation of dCTPαS opposite Gua, dCTPαS opposite 8-oxoGua, and dATPαS opposite 8-oxoGua, respectively.

With pol II$^-$ and unmodified 12/16-mer, substitution of dCTP with dCTPαS decreased the rate of product formation (Figure 1D). The same observation was made for the incorporation of dCTPαS or dATPαS opposite 8-oxoGua-modified 12/16-mer (Figure 1E,F). Elemental effects with pol II$^-$ were ~17, ~31, and ~67 for incorporation of dCTPαS opposite Gua, dCTPαS opposite 8-oxoGua, and dATPαS opposite 8-oxoGua, respectively.

Active Site Titration of Enzyme−DNA Complex. The DNA concentration dependence for formation of active enzyme−DNA complex is shown in Figure 2. KF$^-$ (31 nM) was preincubated with increasing concentrations (12 to 177 nM) of either unmodified 12/16-mer or 8-oxoGua-modified 12/16-mer (Figure 2A). Extension reactions were initiated by the addition of a solution of 200 μM dCTP in buffer A. The concentration of productive KF$^-$−DNA complex increased with increasing concentration of DNA in a manner independent of the presence of Gua or 8-oxoGua in the 16-mer template. The solid lines are the fit of the data to the quadratic equation $K_d = ([E_T - D{\cdot}E][D_T - D{\cdot}E])/[D{\cdot}E]$ for formation of a productive E·D complex ($E + D \rightleftharpoons E{\cdot}D$). The K_d for binding unmodified 12/16-mer (9 ± 3 nM) is similar to the K_d for binding 8-oxoGua-modified 12/16-mer (15 ± 9 nM).

Pol II$^-$ (23 nM) was preincubated with increasing concentrations (12−128 nM) of either unmodified 12/16-mer or 8-oxoGua 12/16-mer, and reactions were initiated by the addition of a solution of 60 μM dCTP in buffer A (Figure 2B). The concentration of productive pol II$^-$−DNA complex increased with increasing concentrations of DNA in the case of unmodified 12/16-mer. When the concentration 8-oxoGua-modified 12/16-mer was increased, the extent of formation of productive pol II$^-$-DNA complex was not as

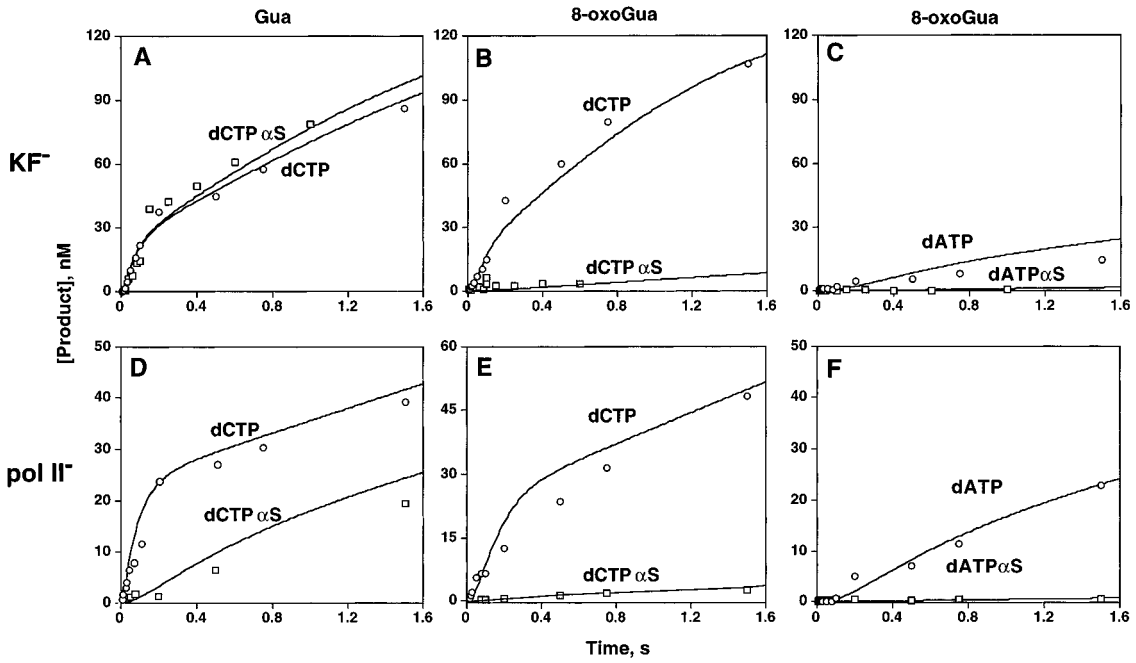

FIGURE 1: Pre-steady-state kinetics of nucleotide incorporation. (A) KF^- (33 nM, preincubated with 128 nM unmodified 12/16-mer) was mixed with a solution of dCTP (30 μM) in buffer A in the rapid quench instrument (○). For analysis of phosphodiester bond formation, KF^- (33 nM, preincubated with 128 nM unmodified 12/16-mer) was mixed with a solution of dCTPαS (92 μM) in buffer A in the rapid-quench instrument (□). All reactions were quenched with 0.3 M EDTA and the data obtained by gel analysis (as described in the Experimental Procedures) were fit by computer simulations. Rate constants obtained from simulations of assays with dCTP are given in Table 3. (B) KF^- (33 nM, preincubated with 128 nM 8-oxoGua-modified 12/16-mer) was mixed with a solution of dCTP (60 μM) in buffer A (○) or with a mixture of dCTPαS (92 μM) in buffer A (□) as described above. (C) KF^- (33 nM, preincubated with 128 nM 8-oxoGua-modified 12/16-mer) was mixed with a solution of dATP (60 μM) in buffer A (○) or with a solution of dATPαS (56 μM) in buffer A (□) as described above. (D) Pol II^- (26 nM, preincubated with 128 nM unmodified 12/16-mer) was mixed with a solution of dCTP (60 μM) (○) or dCTPαS (200 μM) in buffer A (□) as described above. (E) Pol II^- (29 nM, preincubated with 127 nM 8-oxoGua-modified 12/16-mer) was mixed with a solution of dCTP (200 μM) (○) or dCTPαS (200 μM) (□) in buffer A as described above. (F) Pol II^- (29 nM, preincubated with 127 nM 8-oxoGua-modified 12/16-mer) was mixed with a solution of dATP (200 μM) (○) or dATPαS (200 μM) (□) in buffer A as described above.

Table 3: Pre-Steady-State Rate Constants[a]

		KF^-			pol II^-		
	k	G:C	8-oxoG:C	8-oxoG:A	G:C	8-oxoG:C	8-oxoG:A
E + D ⇌ ED	+1	10^8	10^8	10^8	10^8	10^8	10^8
	−1	0.06	0.06	0.06	0.06	0.06	0.06
ED + N ⇌ EDN	+2	10^8	10^8	10^8	10^8	10^8	10^8
	−2	10^3	10^4	10^6	10^2	10^5	10^6
EDN ⇌ XDN	+3	25−75	25−100	50	150	150	150
	−3	6.5	6.5	6.5	6.5	6.5	6.5
XDN ⇌ XFP	+4	1000	25−100	15	100	10	7.5
	−4	0.003	0.003	0.003	0.003	0.003	0.003
XFP ⇌ EFP	+5	>500	>500	>500	>500	>500	>500
	−5	1.4×10^{-4}	1.4×10^{-4}	1.4×10^{-4}	1.4×10^{-4}	1.4×10^{-4}	1.4×10^{-4}
EFP ⇌ EF + P	+6	10^4	10^4	10^4	10^4	10^4	10^4
	−6	10^8	10^8	10^8	10^8	10^8	10^8
EF ⇌ E + F	+7	2	3	0.5	1−2.5	0.75	0.5
	−7	1.2×10^7	1.2×10^7	1.2×10^7	1.2×10^7	1.2×10^7	1.2×10^7

[a] Data were modeled using the kinetic simulation program HopKINSIM as described in the Experimental Procedures. Abbreviations are the same as those used in Scheme 1 with the substitutions X = E*, F = D_{n+1}, and P = PP_i. All values are expressed in units of s^{-1} or M^{-1} s^{-1}. See text for discussion.

great as with the unmodified 12/16-mer. Nevertheless, the K_d for binding unmodified 12/16-mer (21 ± 4 nM, determined as described above for KF^-) is similar to the K_d for binding 8-oxoGua modified 12/16-mer (20 ± 10 nM).

Determination of K_d and k_p for Incorporation of dCTP Opposite Gua and 8-oxoGua. The dNTP dependence of product formation was monitored in progress curves (Figure 3 and data not shown). The solid lines represent a fit of the data to Scheme 1 and the rate constants shown in Table 3. Progress curves for the data not shown for addition of dATP opposite 8-oxoGua by KF^- and for all three cases with pol II^- were also used in mathematical simulations with KINSIM to delineate the rate constants for stepwise polymerization (Table 3).

In order to estimate K_d and k_p, the burst phase portions of the progress curves for dCTP addition opposite Gua and 8-oxoGua were expanded to provide more data points in the single-turnover region (data not shown). The rates of product formation in the burst phase (k_p), single-turnover portion of the curves were determined by first order (single-exponential) analysis. This was accomplished by plotting $\ln(P_n - P_t)$ against t to yield lines which have slopes of $-k_{obs}$, where P_n

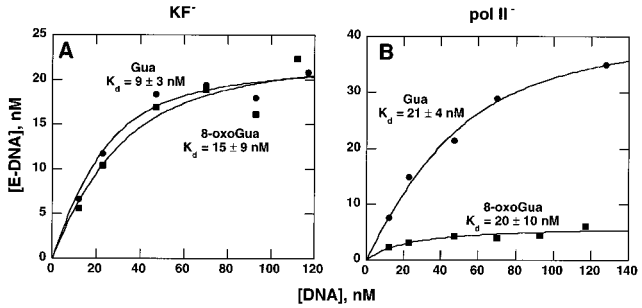

FIGURE 2: Active-site titration of E·DNA. (A) KF^- (31 nM) was preincubated with varying concentrations of either 8-oxoGua-modified (■) or unmodified (●) 12/16-mer (12, 23, 47, 70, 93, and 117 nM) and then mixed with a solution of dCTP (200 μM) in buffer A. Resulting burst amplitudes for each concentration of DNA were determined and plotted against [DNA] as shown. The solid lines are the fit of the data to the quadratic equation $[E{\cdot}D] = 0.5\text{-}(K_d + E_t + D_t) - [0.25(K_d + E_t + D_t)^2 - (E_tD_t)]^{1/2}$, where E_t = [total enzyme], D_t = [total DNA], and K_d = dissociation constant for the reaction $E + D \rightleftharpoons E{\cdot}D$. The K_d values for KF^- binding unmodified (9 ± 3 nM) and 8-oxoGua-modified (15 ± 9 nM) 12/16-mer are considered not to differ. (B) Pol II^- (21 nM) was preincubated with varying concentrations of DNA and dCTP as described above. The K_d values for pol II^- binding of unmodified (●) (21 ± 4 nM) and 8-oxoGua-modified (■) (20 ± 10 nM) 12/16-mer are considered not to differ.

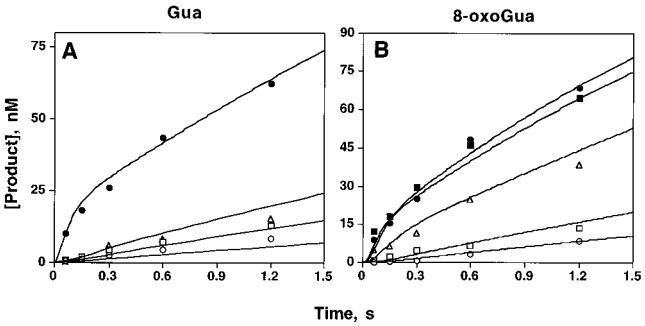

FIGURE 3: Dependence of KF^- pre-steady state progress curves on dNTP concentration. (A) KF^- (19−26 nM), preincubated with 128 nM unmodified 12/16-mer, was mixed with increasing concentrations of dCTP (0.2 μM, ○; 0.4 μM, □; 0.8 μM, △; 20 μM, ●) in buffer A. Products were analyzed by gel electrophoresis as described in the Experimental Procedures. Resulting product burst curves were fitted by mathematical simulations using KINSIM. The solid lines represent a fit of the data to the mechanism in Scheme 1 and the rate constants in Table 3. (B) KF^- (19−27 nM), preincubated with 116 nM 8-oxoGua-modified 12/16-mer, was mixed with increasing concentrations of dCTP (5 μM, ○; 10 μM, □; 20 μM, △; 60 μM, ●; 200 μM, ■) in buffer A. The data were analyzed as described above.

is the concentration of product at the end of the burst phase, P_t is the concentration of product at time t in the burst phase, and k_{obs} is the observed rate of the burst reaction. These rates (k_{obs}) were then plotted against [dCTP] and fitted to the hyperbola $k_{obs} = \{k_p[dCTP]/([dCTP] + K_d)\}$, which describes the reaction equation

$$E{\cdot}D + N \overset{K_d}{\rightleftharpoons} E{\cdot}D{\cdot}N \overset{k_p}{\rightleftharpoons} E{\cdot}D_{n+1}{\cdot}PP_i$$

where E = enzyme, D = 12/16-mer oligomer, N = dCTP, D_{n+1} = 13/16-mer product oligomer, and PP_i = pyrophosphate. In order to determine the k_p values for KF^- and pol II^- insertion of dATP opposite 8-oxoGua (where no burst is observed), the slopes of the time progress curves (Figure 1, panels C and F, respectively) were divided by the final concentration of enzyme (Kati *et al.*, 1992). The K_d for binding of dATP was determined by competition assays described later.

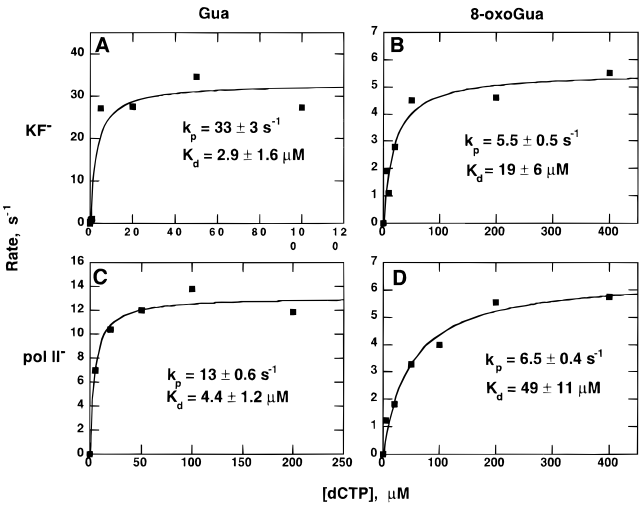

FIGURE 4: Determination of K_d and k_p. (A) KF^- (35−50 nM), preincubated with 103 nM unmodified 12/16-mer, was mixed with increasing concentrations of dCTP (1−100 μM) in buffer A over a time range varying from 15 to 300 ms. The pre-steady-state rates of product formation were determined by single-exponential analysis of the burst phase (see text for explanation) and then plotted against the dCTP concentrations to determine the K_d and k_p for incorporation of dCTP in the unmodified 12/16-mer (■) by KF^-. The solid line represents the fit of the rate data to the hyperbola $k_{obs} = \{k_p[dCTP]/([dCTP] + K_d)\}$. (B) KF^- (35−50 nM), preincubated with 103 nM 8-oxoGua-modified 12/16-mer, was mixed with increasing concentrations of dCTP (5−400 μM) in buffer A over a time range varying from 25 to 600 ms. The pre-steady-state rates of product formation were determined by single-exponential analysis of the burst phase and then were plotted against the dCTP concentrations to determine the K_d and k_p for incorporation of dCTP in the 8-oxoGua-modified 12/16-mer (■) by KF^-. The solid line represents the fit of the rate data to the hyperbola $k_{obs} = \{k_p[dCTP]/([dCTP] + K_d)\}$. (C) Pol II^- (27−33 nM) was preincubated with 103 nM unmodified 12/16-mer and then mixed with increasing concentrations of dCTP (1−200 μM) in buffer A over a time range varying from 15 to 300 ms. The pre-steady-state rates of product formation were determined by single-exponential analysis of the burst phase and then were plotted against the dCTP concentrations to determine the K_d and k_p for incorporation of dCTP in the unmodified 12/16-mer (■) by pol II^-. The solid line represents the fit of the rate data to the hyperbola $k_{obs} = \{k_p[dCTP]/([dCTP] + K_d)\}$. (D) Pol II^- (41−47 nM) was preincubated with 112 nM 8-oxoGua-modified 12/16-mer and then mixed with increasing concentrations of dCTP (5−400 μM) in buffer A over a time range varying from 25 to 600 ms. The pre-steady-state rates of product formation were determined by single-exponential analysis of the burst phase and then were plotted against the dCTP concentrations to determine the K_d and k_p for incorporation of dCTP in the 8-oxoGua-modified 12/16-mer (■) by pol II^-. The solid line represents the fit of the rate data to the hyperbola $k_{obs} = \{k_p[dCTP]/([dCTP] + K_d)\}$.

The curves for KF^- incorporation of dCTP opposite Gua or 8-oxoGua were used to determine K_d for dCTP binding and k_p (rate of product formation) as described above (Figure 4A,B and Table 4). The KF^- k_p values for incorporation of dCTP opposite either Gua or 8-oxoGua differ by 6−7-fold (33 ± 3 s^{-1} and 5.5 ± 0.6 s^{-1}, respectively), and there is a ~6-fold difference in the K_d values (3.2 ± 1.1 μM for incorporation opposite Gua and 19 ± 7 μM for incorporation opposite 8-oxoGua). The k_p for insertion of dATP opposite 8-oxoGua by KF^- was estimated to be ~0.3 s^{-1} by the method described above (Table 4).

Curves for pol II^- incorporation of dCTP opposite Gua or 8-oxoGua were used to determine K_d for dCTP binding and k_p as described above (data not shown). The pol II^- k_p values for incorporation of dCTP opposite either Gua or 8-oxoGua differ by a factor of 2 (13.1 ± 0.6 s^{-1} and 6.6 ±

Table 4: Pre-Steady-State Kinetic Parameters for KF$^-$ and Pol II$^-$

	KF$^-$		pol II$^-$	
	K_d (μM)	k_p (s^{-1})	K_d (μM)	k_p (s^{-1})
G:C[a]	3.2 ± 1.1	33 ± 3	4.4 ± 1.2	13.1 ± 0.6
8-oxoG:C[a]	19 ± 7	5.5 ± 0.6	49 ± 11	6.6 ± 0.8
8-oxoG:A[a]	~190[b]	~0.3[c]	~150[b]	~0.4[c]

[a] The base in the oligomer is presented first (G or 8-oxoG), followed by the dNTP used (C or A). [b] Estimates based on competition assays containing dCTP and dATP. See Figures 6 and 7 and text for discussion. [c] Estimates made by dividing the slope of the progress curves (Figure 1C,F) by the enzyme concentration.

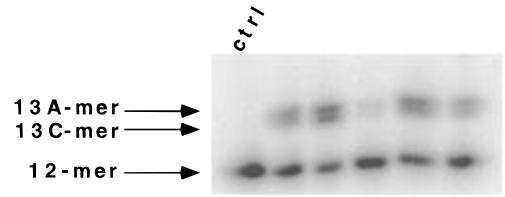

FIGURE 5: Separation of 12-mer primer extended by either C or A. The 13-mer products of the competition assays were resolved by electrophoresis in 20% acrylamide/8 M urea and bands were quantitated as described in Experimental Procedures.

0.8 s^{-1}, respectively), and there is an order of magnitude difference in the K_d values (4.4 ± 1.2 μM for incorporation opposite Gua and 49 ± 11 μM for incorporation opposite 8-oxoGua) (Figure 4C,D and Table 4). The k_p for insertion of dATP opposite 8-oxoGua by pol II$^-$ was estimated to be ~0.5 s^{-1} by the method described above (Table 4).

Determination of $K_{d,app}$ for Incorporation of dATP Opposite 8-oxoGua by Competition Assays with dCTP. In order to estimate the apparent binding affinity of polymerase for dATP, competition assays with dCTP were performed. These assays provided a measure of the dNTP binding which lead to incorporation and do not necessarily reflect nonproductive, total binding. The assays were done using the general approach described in Experimental Procedures for the rapid-quench experiments, except that the dNTP solution contained both dCTP and dATP. Due to the slower migration of primer extended by A, the product bands corresponding to extension by C and A could be resolved on 20% acrylamide/8.0 M urea gels (Figure 5).

The progress curves for competition of dCTP by dATP with KF$^-$ are shown for a dCTP concentration of 20 μM and dATP concentrations of 20, 60, and 200 μM (Figure 6, panels A, B, and C, respectively). When the concentration of dATP was ~10-fold higher than the concentration of dCTP, the rates of product formation were similar. This result suggests that the $K_{d,app}$ for binding of dATP is ~10-fold higher than that for binding dCTP (Table 4). Experiments were also done with the concentration of dCTP held at 60 μM while the concentration of dATP was varied, as described above, and with dCTP and dATP concentrations of 200 μM (results not shown). Those experiments were in agreement with the ~10-fold higher $K_{d,app}$ for KF$^-$ binding of dATP over dCTP.

Progress curves for competition of dCTP by dATP with pol II$^-$ are shown for a dCTP concentration of 20 μM and dATP concentrations of 20, 60, and 200 μM (Figure 7, panels A, B, and C, respectively). For pol II$^-$, the $K_{d,app}$ for binding dATP is ~3-fold higher than dCTP (Table 4). Experiments were also done with the concentration of dCTP held at 60 μM while the concentration of dATP was varied, as described above, and with dCTP and dATP concentrations of 200 μM (results not shown). Those experiments were in agreement with the ~3-fold higher $K_{d,app}$ for pol II$^-$ binding of dATP over dCTP.

Addition of the Next Correct Base Following a C:8-OxoGua or A:8-OxoGua Base Pair. Previously, Shibutani et al. (1991) found with KF$^+$ that extension past a C:8-oxoGua mispair was slow while extension of an A:8-oxoGua mispair occurred readily. The findings from those steady-state experiments were confirmed in the present study with both KF$^-$ and pol II$^-$ using pre-steady-state approaches, in the sequence context defined in Table 1. The general approach for the extension experiments is outlined in Scheme 2. Enzyme was preincubated with unmodified 16-mer annealed to either a 13C- or 13A-primer (Table 1) such that a C:G or an A:G base pair was formed, respectively. To initiate reactions, the preincubated solution of enzyme−DNA was rapidly mixed with a solution of the next correct nucleotide (dGTP, 200 μM) plus $MgCl_2$. Both KF$^-$ and pol II$^-$ were able to efficiently extend the C:G and A:8-oxoGua base pairs while extension of the A:G mispair or the C:8-oxoGua base pair was blocked (Figure 8).

DISCUSSION

In order to comprehend how DNA adducts are misreplicated and correctly replicated, it is necessary to understand the kinetics of stepwise polymerization as related to the structures of modified base pairs containing DNA adducts and to the polymerases involved in replication (Johnson, 1993). In the present study, kinetic analysis of the replication of 8-oxoGua by the model enzymes KF$^-$ and pol II$^-$ was done in an effort to delineate how individual steps in polymerization contribute to dNTP incorporation opposite the lesion. The most notable differences between replication of the unmodified 12/16-mer as opposed to replication of the 8-oxoGua-modified 12/16-mer occurred at the levels of nucleotide binding, phosphodiester bond formation, and efficiency of base pair extension.

Analysis of the replication of 8-oxoGua compared to Gua in a defined sequence began with steady-state assays to measure the kinetic parameters K_m and k_{cat} for insertion of C opposite Gua and 8-oxoGua and of A opposite 8-oxoGua. There has been considerable discussion concerning the meaning of k_{cat} and K_m steady-state parameters in polymerase systems. Due to the complexity of the mechanism of polymerization (Scheme 1), k_{cat} does not provide an accurate measurement of the rate of nucleotide incorporation, particularly in standing start assay conditions, i.e., only one nucleotide incorporated. Indeed, all measured pre-steady-state parameters, especially k_p, are greater than steady-state k_{cat} values for both polymerases (Tables 2 and 4). The differences between steady-state and pre-steady-state kinetic parameters result because the steady-state k_{cat} value is dominated by the slow rate for dissociation of the DNA from these processive polymerases, which causes the apparent K_m and k_{cat} values from steady-state analysis to be smaller than the pre-steady-state kinetic parameters K_d and k_p (Kati et al., 1992). The advantage of pre-steady-state kinetic analysis, then, is that the rate of polymerization and K values can be measured without interference from the rates of dissociation and association of the DNA (Kati et al., 1992).

The results of pre-steady-state time course reactions (Figure 1) show a burst of product formation in the cases where dCTP is added opposite Gua or 8-oxoGua. This

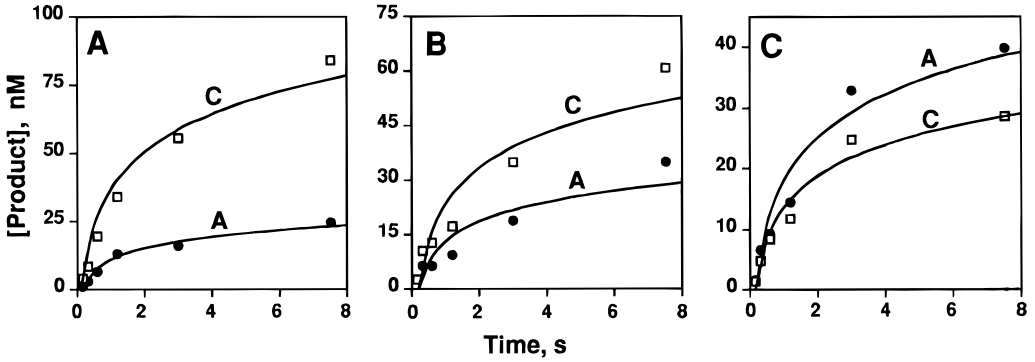

FIGURE 6: Estimation of $K_{d,app}$ for KF^- binding of dATP in presence of 8-oxoGua oligomer. Competition assays were carried out with 39 nM KF^-, 129 nM 8-oxoGua-modified 12/16-mer, 20 μM dCTP, and varying concentrations of dATP. Extension of the primer by C (□) or A (●) is indicated. The solid lines represent single-exponential fits (which, as shown, do not necessarily go through the origin). (A) [dATP] = 20 μM. (B) [dATP] = 60 μM. (C) [dATP] = 200 μM.

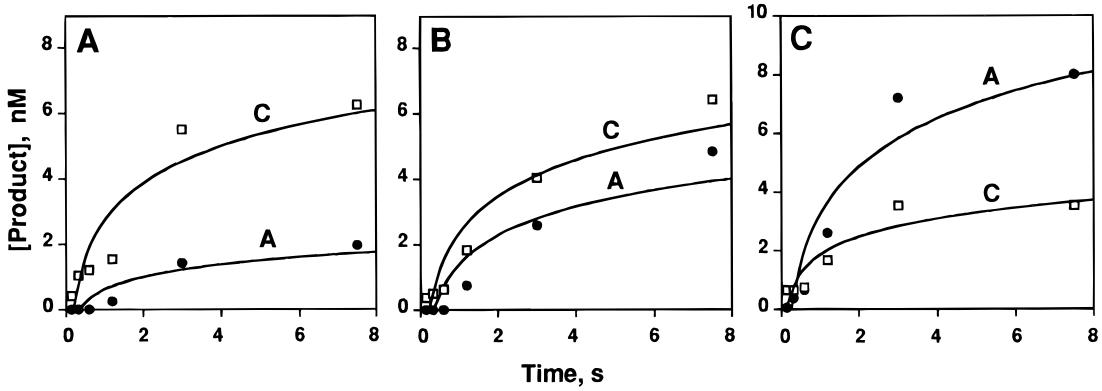

FIGURE 7: Estimation of $K_{d,app}$ for pol II^- binding of dATP in presence of 8-oxoGua oligomer. Competition assays were carried out with 21 nM pol II^-, 131 nM 8-oxoGua-modified 12/16-mer, 20 μM dCTP, and varying concentrations of dATP. Primer extended by C (□) or A (●) is indicated. The solid lines represent single-exponential fits (which, as shown, do not necessarily go through the origin). (A) [dATP] = 20 μM. (B) [dATP] = 60 μM. (C) [dATP] = 200 μM.

Scheme 2: Extension of A:8-oxoGua and C:8-oxoGua Base Pairs

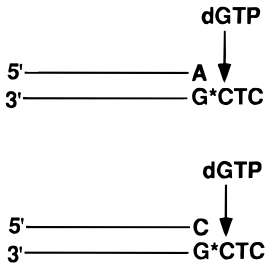

G* = Gua or 8-oxoGua

suggests that the rate-limiting step for dCTP incorporation occurs after the chemistry step (Johnson, 1993). Conversely, in the cases where dATP is added opposite 8-oxoGua, there is no burst of product formation suggesting that the rate-limiting step must occur at or before the chemical step. Elemental substitutions were done with dNTPαS analogs of the normal dNTPs in order to examine these findings further (Figure 1). Although it is uncertain to what extent elemental (thio) analysis can be interpreted in measuring the rate-limiting nature of phosphodiester bond formation [for discussion of this issue, see Reardon (1992) and Tan et al. (1994)], such analysis clearly showed that chemistry is not rate-limiting for addition of dCTP opposite Gua for KF^-, in agreement with previous studies of the mechanism of KF^- (Kuchta et al., 1988; Eger & Benkovic, 1992). However, for addition of C or A opposite 8-oxoGua, chemistry appears to be rate-limiting as suggested by the elemental effects of ~35 and ~20, respectively. Since addition of dCTP opposite 8-oxoGua displays similar burst kinetics to the control case (dCTP opposite Gua), it is possible that chemistry is only partially rate-limiting. The dNTPαS studies with pol II^- suggest that chemistry is a rate-limiting factor for all three cases (i.e., addition of dCTP opposite Gua or 8-oxoGua and the addition of dATP opposite 8-oxoGua), since the elemental effects were determined to be ~17, ~31, and ~67, respectively. This appears to be the first time a moderate elemental effect for the addition of the correct nucleotide opposite an unmodified base by a polymerase has been reported in the literature and suggests kinetic divergence for pol II^- relative to other polymerases.

The results of the pre-steady-state active site titrations of KF^- and pol II^- show that neither polymerase discriminates between unmodified and 8-oxoGua-modified 12/16-mer substrates in binding (Figure 2). However, there is a difference in curve amplitude for Gua- and 8-oxoGua-containing 12/16-mers for the pol II^- active site titrations. The concentration of E·DNA species does not increase much as the concentration of DNA is increased. The dNTP dependence curves show that KF^- does discriminate in binding dCTP when incorporation is opposite 8-oxoGua compared to Gua (K_d 19 ± 7 μM vs K_d 3.2 ± 1.1 μM) (Figure 4). The trend is the same with pol II^-, where the K_d for addition of dCTP opposite Gua was 4.4 ± 1.2 μM while opposite 8-oxoGua the K_d was 51 ± 17 μM (Figure 4). For both enzymes, however, the k_p values for addition of dCTP opposite Gua and 8-oxoGua varied. Also, the k_p values for addition of dCTP opposite 8-oxoGua were similar

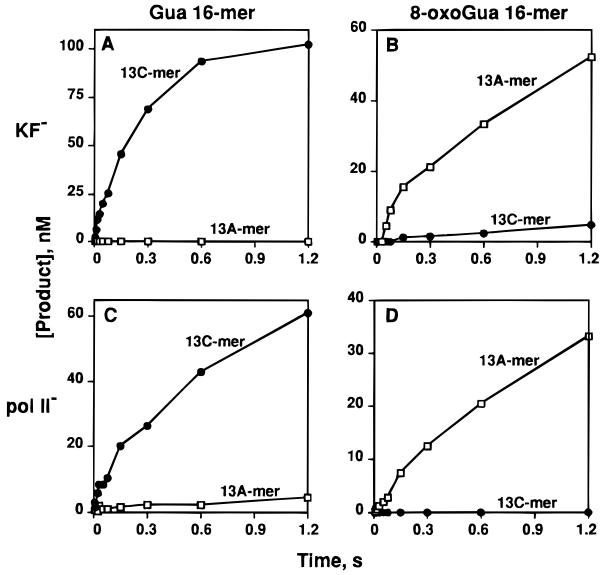

FIGURE 8: Extension past C:G, C:8-oxoGua, A:G, and A:8-oxoGua base pairs. Refer to Scheme 2 for design of experiment. (A) KF^- (57 nM) was preincubated with unmodified template annealed to either a 13C (●) or 13A (□) primer (116 nM) such that a C:G or a A:G base pair was formed, respectively. Extension reactions were initiated by the addition of a solution of 200 μM dGTP in buffer A. (B) KF^- (57 nM) was preincubated with 8-oxoGua-modified template annealed to either a 13C (●) or 13A (□) primer (116 nM) such that a C:8-oxoGua or a A:8-oxoGua base pair was formed, respectively. Extension reactions were initiated by the addition of a solution of 200 μM dGTP in buffer A. (C) Pol II^- (32 nM) was preincubated with unmodified template annealed to either a 13C (●) or 13A (□) primer (123 nM) such that a C:G or a A:G base pair was formed, respectively. Extension reactions were initiated by the addition of a solution of 200 μM dGTP in buffer A. (D). Pol II^- (32 nM) was preincubated with 8-oxoGua-modified template annealed to either a 13C (●) or 13A (□) primer (123 nM) such that a C:8-oxoGua or a A:8-oxoGua base pair was formed, respectively. Extension reactions were initiated by the addition of a solution of 200 μM dGTP in buffer A.

for both enzymes as were the k_p values for addition of dATP opposite 8-oxoGua.

Since the addition of dATP opposite 8-oxoGua did not display burst kinetics with either polymerase, estimates of $K_{d,app}$ and k_p had to be made by methods other than dNTP dependence curves. An estimate of k_p was provided by dividing the slope of the time course curve by the concentration of enzyme (Table 4) (Kati *et al*., 1992). Again, the k_p values were greater than steady-state k_{cat} values (Table 4). The $K_{d,app,dATP}$ was estimated from competition assays with dATP and dCTP (Figures 6 and 7). From these assays, the $K_{d,app,dATP}$ was shown to be ~10-fold higher than the $K_{d,dCTP}$ for incorporation opposite 8-oxoGua by KF^- (Figure 6). In the case of pol II^-, the $K_{d,app,dATP}$ was only ~3-fold higher than the $K_{d,dCTP}$ (Figure 7). Thus, the $K_{d,app}$ values for addition of dATP opposite 8-oxoGua were estimated to be ~190 and ~150 μM by KF^- and pol II^-, respectively (Table 4). These $K_{d,app}$ values, while considerably larger than those determined from steady-state analysis (1.7 ± 1.3 μM and 11 ± 1 μM for KF^- and pol II^-, respectively) (Table 2), are simliar.

In the type of analysis done in the present study we are able to measure only productive binding of dNTPs, i.e., binding that results in incorporation and measurable product formation. Since all binding does not lead to product formation, the high $K_{d,app,dATP}$ values may partially result from contributions of a slow conformational change and/or a slow rate of phosphodiester bond formation. That is, K_d and k_p are more complex constants which cannot be simply equated with k_{-2}/k_2 and k_4, respectively. A physical approach, e.g., fluorescence quenching, is needed to better define true K_d values for addition of dNTPs and to delineate the individual contributions of the polymerase, the oligonucleotide, and the conformational changes to K_d.

Using the dNTP dependence curves for fitting, a set of rate constants governing polymerization (Scheme 1) were determined by mathematical analysis using the kinetic simulation program KINSIM (Table 3). Rate constants presented in Table 3 were determined by simulations of experiments where a single nucleotide was presented for incorporation, either dCTP or dATP (rate constants for incorporation of thio analogs were also determined but are not shown). This type of analysis has been used to provide quantitative estimates of the rate constants governing the mechanism of polymerization by KF^+, T7 DNA polymerase, and HIV-1 reverse transcriptase (Eger & Benkovic, 1992; Kuchta et al., 1988; Wong et al., 1991; Patel et al., 1991; Kati et al., 1992). Initial estimates of rate constants for KINSIM simulations of the dNTP dependence curves and progress curves were obtained from previous analysis of KF^+ (Eger & Benkovic, 1992; Tan et al., 1994). Adjustments were then made to fit the data for pre-steady-state kinetic parameters presented in this paper for the oligonucleotide sequences shown in Table 1 and for the enzymes used, KF^- and pol II^-. The rate constants most sensitive to change for burst analysis include those for steps 1, 2, 3, and 4, while the forward and reverse rate constants for step 7 are most sensitive in describing the rate of multiple turnovers. For the incorporation of dATP by either KF^- or pol II^-, k_2 and k_4 are the most sensitive rate constants. In all cases where addition occurs opposite 8-oxoGua, k_4 becomes at least partially rate-limiting, consistent with the results of the thio substitution assays. Also, elemental effects (Figure 1) suggest that in the case of addition of dCTP opposite Gua by pol II^- chemistry is at least partially rate-limiting, and this result is reflected in estimates of k_4 from the KINSIM simulations (Table 3).

On the basis of simulations with KINSIM and the dNTP dependence curves, it appears that in general the mechanism of pol II^- is the same as that reported for $KF^{+/-}$, T7 DNA polymerase, and HIV-1 reverse transcriptase (Kuchta et al., 1988; Wong et al., 1991; Eger & Benkovic, 1992; Patel et al., 1991; Kati et al., 1992) (Scheme 1). There are some differences to note, however, between the kinetics of pol II^- and KF^- replication of 8-oxoGua. First, in steady-state assays with pol II^- the K_m and k_{cat} values for insertion of dCTP or dATP opposite 8-oxoGua are similar to each other but different from the values for insertion of dCTP opposite Gua. In contrast, with KF^- the K_m values for insertion of dCTP opposite Gua and dATP opposite 8-oxoGua are similar to each other but dissimilar from the K_m for insertion of dCTP opposite 8-oxoGua. Also, with KF^- the k_{cat} values for insertion of dCTP opposite Gua or 8-oxoGua are similar to each other while the k_{cat} for insertion of dATP opposite 8-oxoGua is two orders of magnitude lower. In the pre-steady-state analysis, discussed above, differences between KF^- and pol II^- were more subtle because the enzymes follow the same trends. The two most apparent differences are in the active site titration experiments where the amplitude of the concentration of pol II^-·8-oxoGua-modified 12/16-mer complex does not match that for the pol

II$^-$·unmodified 12/16-mer complex and in the phosphorothioate substitution reactions where a moderate elemental effect is seen with pol II$^-$. Another difference between the enzymes is noted in the increased mutation frequency seen with pol II$^-$ reflected both in steady-state determination of the apparent misinsertion frequency and in pre-steady-state estimates of the K_d for productive binding of dATP from competition assays. Also, the increased misinsertion frequency of pol II$^-$ relative to KF$^-$ is noted in the ratio $[(k_p/K_d)_{wrong}/(k_p/K_d)_{right}]$.

As eluded to earlier, the structures of base pairs containing DNA adducts play an important role in determining the mutagenicity of a DNA modification. On the basis of X-ray crystallographic and NMR structural analyses of 8-oxoGua base pairs with A and C, the A:8-oxoGua base pair resembles an A:T Watson−Crick base pair (Kouchakdjian et al., 1991; McAuley-Hecht et al., 1994; Lipscomb et al., 1995). The observation of the similarity of A:8-oxoGua to a Watson−Crick base pair has lead to the suggestion that the mutagenicity of 8-oxoGua results from its ability to form a Watson−Crick-like base pair with A (Kouchakdjian et al., 1991; McAuley-Hecht et al., 1994; Lipscomb et al., 1995). In the case of normal base mismatches, i.e., in the absence of adducts, the next base addition following the mismatch is very slow compared to base addition following a Watson−Crick base pair (Echols & Goodman, 1991). Shibutani et al. (1991) reported that the "mismatch" A:8-oxoGua base pair is readily extended while the "correct" pair of C:8-oxoGua is not. This result was confirmed using single nucleotide incorporation techniques in the present study (Figure 8). Since the A:8-oxoGua pair does not block replication, the polymerase will continue to replicate the DNA allowing the miscoded residue to remain and be passed on to the daughter cell if the mismatch is not recognized and repaired by cellular repair mechanisms.

In conclusion, part of the mutagenicity of DNA adducts results from the ability of DNA polymerases to incorporate an incorrect nucleotide opposite an adduct displaying appropriate structural and base-pairing qualities to allow for efficient incorporation and extension. Fidelity has been shown here to be dependent on several distinct factors including nucleotide binding, phosphodiester bond formation, and efficiency of base pair extension.

ACKNOWLEDGMENT

We thank Dr. Kevin Raney for helpful discussions during the preparation of the manuscript and Dr. Carl Frieden for supplying the KINSIM program and technical advice in its use.

REFERENCES

Ames, B. N., & Gold, L. S. (1991) *Mutat. Res. 250*, 3−16.
Ames, B. N., Shigenaga, M. K., & Gold, L. S. (1993) *Environ. Health Perspect. 101 (Suppl. 5)*, 35−44.
Barshop, B. A., Wrenn, R. F., & Frieden, C. (1983) *Anal. Biochem. 130*, 134−145.
Basu, A. K., & Essigmann, J. M. (1988) *Chem. Res. Toxicol. 1*, 1−18.
Basu, A. K., & Essigmann, J. M. (1990) *Mutat. Res. 233*, 189−201.
Bodepudi, V., Shibutani, S., & Johnson, F. (1992) *Chem. Res. Toxicol. 5*, 608−617.
Boosalis, M. S., Petruska, J., & Goodman, M. F. (1987) *J. Biol. Chem. 262*, 14689−14696.
Boosalis, M. S., Mosbaugh, D. W., Hamatake, R., Sugino, A., Kunkel, T. A., & Goodman, M. F. (1989) *J. Biol. Chem. 264*, 11360−11366.
Boyer, P. N. (1975) in *Handbook of Biochemistry and Molecular Biology* (Fasman, G. D., Ed.) 3rd ed., p 589, CRC Press, Cleveland, OH.
Bryant, F. R., Johnson, K. A., & Benkovic, S. J. (1983) *Biochemistry 22*, 3537−3546.
Cai, H., Yu, H., McEntee, K., Kunkel, T. A., & Goodman, M. F. (1995) *J. Biol. Chem. 270*, 15327−15335.
Cheng, K. C., Cahill, D. S., Kasai, H., Nishimura, S., & Loeb, L. A. (1992) *J. Biol. Chem. 267*, 166−172.
Derbyshire, V., Freemont, P. S., Sanderson, M. R., Beese, L., Freidman, J. M., Joyce, C. M., & Steitz, T. A. (1988) *Science 240*, 199−201.
Echols, H., & Goodman, M. F. (1991) *Annu. Rev. Biochem. 60*, 477−511.
Eger, B. T., & Benkovic, S. J. (1992) *Biochemistry 31*, 9227−9236.
Eger, B. T., Kuchta, R. D., Carroll, S. S., Benkovic, P. A., Dahlberg, M. E., Joyce, C. M., & Benkovic, S. J. (1991) *Biochemistry 30*, 1441−1448.
Feig, D. I., & Loeb, L. A. (1994) *J. Mol. Biol. 235*, 33−41.
Johnson, K. A. (1992) in *The Enzymes* (Boyer, P. D., Ed.) pp 1−61, Academic Press, Inc., New York.
Johnson, K. A. (1993) *Annu. Rev. Biochem. 62*, 685−713.
Joyce, C. M., & Grindley, N. D. F. (1983) *Proc. Natl. Acad. Sci. U.S.A. 80*, 1830−1834.
Kati, W. M., Johnson, K. A., Jerva, L. F., & Anderson, K. S. (1992) *J. Biol. Chem. 267*, 25988−25997.
Kornberg, A., & Baker, T. A. (1992) *DNA Replication*, 2nd ed., W. H. Freeman and Co., New York.
Kouchakdjian, M., Bodepudi, V., Shibutani, S., Eisenberg, M., Johnson, F., Grollman, A. P., & Patel, D. J. (1991) *Biochemistry 30*, 1403−1412.
Kuchta, R. D., Benkovic, P., & Benkovic, S. J. (1988) *Biochemistry 27*, 6716−6725.
Laemmli, U. K. (1970) *Nature 227*, 680−685.
Lindsley, J. E., & Fuchs, R. P. P. (1994) *Biochemistry* 33, 764−772.
Lipscomb, L. A., Peek, M. E., Morningstar, M. L., Verghis, S. M., Miller, E. M., Rich, A., Essigmann, J. M., & Williams, L. D. (1995) *Proc. Natl. Acad. Sci. U.S.A. 92*, 719−723.
Malins, D. C., & Haimanot, R. (1991) *Cancer Res. 51*, 5430−5432.
Malins, D. C., Homes, E. H., Polissar, N. L., & Gunselman, S. J. (1993) *Cancer 71*, 3036−3043.
Malins, D. C., Polissar, N. L., Nishikida, K., Homes, E. H., Gardner, H. S., & Gunselman, S. J. (1995) *Cancer 75*, 503−517.
Marnett, L. J., & Burcham, P. C. (1993) *Chem. Res. Toxicol. 6*, 771−785.
McAuley-Hecht, K. E., Leonard, G. A., Gibson, N. J., Thomson, J. B., Watson, W. P., Hunter, W. N., & Brown, T. (1994) *Biochemistry 33*, 10266−10270.
Patel, S. S., Wong, I., & Johnson, K. A. (1991) *Biochemistry 30*, 511−525.
Reardon, J. E. (1992) *Biochemistry 31*, 4473−4479.
Shibutani, S., Takeshita, M., & Grollman, A. P. (1991) *Nature 349*, 431−434.
Shimoda, R., Nagashima, M., Sakamoto, M., Yamaguchi, N., Hirohashi, S., Yokota, J., & Kasai, H. (1994) *Cancer Res. 54*, 3171−3172.
Takeuchi, T., Nakajima, M., Ohta, Y., Mure, K., Takeshita, T., & Morimoto, K. (1994) *Carcinogenesis 15*, 1519−1523.
Tan, H. B., Swann, P. F., & Chance, E. M. (1994) *Biochemistry 33*, 5335−5346.
Wong, I., Patel, S. S., & Johnson, K. A. (1991) *Biochemistry 30*, 526−537.

BI960485X